Available at
http://pvamu.edu/aam
Appl. Appl. Math.
ISSN: 1932-9466

Applications and Applied Mathematics:
An International Journal
(AAM)

Special Issue No. 2 (May 2016), pp. 9 – 21
18th International Mathematics Conference, March 20 – 22, 2014, IUB Campus, Bashundhara Dhaka, Bangladesh

Effect of Solid Volume Fraction on Forced Convective Flow of Nanofluid through Direct Absorption Solar Collector

Salma Parvin*, Rehena Nasrin and M.A. Alim

Department of Mathematics
Bangladesh University of Engineering and Technology
Dhaka-1000, Bangladesh
*E-mail: salpar@math.buet.ac.bd

ABSTRACT

The present work numerically investigates the heat transfer performance and entropy generation of forced convection through a direct absorption solar collector. The working fluid is Cu-water nanofluid. The simulations focus specifically on the effect of solid volume fraction of nanoparticle on the mean Nusselt number, total entropy generation, Bejan number and collector efficiency. Also Isotherms, heat function and entropy generation are presented for various solid volume fraction. The governing partial differential equations are solved using penalty finite element method with Galerkins weighted residual technique. The results show that the mean Nusselt number and mean entropy generation increases as the volume fraction of Cu nanoparticles increases. The results presented in this study provide a useful source of reference for enhancing the force convection heat transfer performance while simultaneously reducing the entropy generation.

KEYWORDS: Forced convection; direct absorption solar collector; finite element method; nanofluid; solid volume fraction

AMS-MSC 2010 No.: 76D05, 80A20

1. INTRODUCTION

The conversion of solar energy into heat is done with the help of solar collectors. Most commonly used collectors are simple in construction and are flat plate type collectors. New classes of collectors which are used to increase the efficiency of the collectors are direct absorption solar collector (DASC) Taylor et al. (2011a). The DASC's were firstly proposed in the mid 1970's but the major problem faced by these collectors was the poor absorption

properties of conventional fluids used in these collectors. By the development of new class of fluids known as nanofluids which show improved properties over the conventional fluids, these type of collectors can gain importance Taylor et al. (2011b). Nanofluids are new class of fluids in which nanometer sized (1-100 nm) particles of metal/nonmetals/metal oxides etc. are dispersed in conventional fluids. Based on DASC, the attempt had been made to investigate the variation in collector efficiency using nanofluids by Verma and Kundan (2013), Tyagi et al. (2009), Otanicar et al. (2010), Mahian et al. (2013). Heat transfer enhancement in solar devices is one of the key issues of energy saving and compact designs. The problem of heat loss, collector efficiency in various solar collectors filled with traditional fluid as well as different nanofluids have attracted significant attention in recent years Zambolin (2011), Nasrin et al. (2014, 2015), Parvin et *al.* (2014), Álvarez et al. (2010), Natarajan and Sathish (2009).

All thermofluidic processes involve irreversibilities and therefore incur an efficiency loss. Inpractice, the extent of these irreversibilities can be measured by the entropy generation rate. In designing practical systems, it is desirable to minimize the rate of entropy generation so as to maximize the available energy Bejan (1996, 1982), Khorasanizadeh (2013), Delavar and Hedayatpour (2012), Parvin and Chamkha (2014). Overall, the results have shown that the rate of entropy generation increases as the irreversibility distribution ratio increase. Moreover, for given values of the irreversibility distribution ratio, the entropy generation rate is determined by the heat transfer irreversibility and/or fluid friction irreversibility. The ‘heat line’ method of visualizing the true path of convection heat transfer was studied by Morega and Bejan (1993), Basak et al. (2010).It was developed as the convection counterpart (or the generalization) of the technique of heat flux lines used routinely in heat conduction.

As nanofluid based solar collectors are not available commercially, so in this section itis going to discuss the assumptions and the choices made in the considered solar collector for this specific application. Commonly used base liquids are water, oil, ethylene glycol etc. The choice between these liquids is determined by the operating temperatures of the solar collectors since, the collector operates between (0°C - 100°C) (i.e., considered as low temperature range solar collector). So, taking this into consideration it has been decided to use distilled water as base fluid, which is cost effective also. In the next step selection of the nanoparticle is done. Although, in market a range of different type of nano-particles in the form of nanopowders is available, but its use for a particular application depends upon the factors like; easy availability, cost and comparatively improved properties. So it has been decided to use Cu nanoparticle for this particular application. The concentration of the nanoparticles in the nanofluids is a very important parameter in the absorption of the solar energy.

In the light of above discussions, it is seen that there has been a good number of works in the field of heat transfer system through a direct-absorption solar collector. In spite of that there is some scope to work with fluid flow, heat transfer, entropy generation and enhancement of collector efficiency using nanofluid. Also temperature distribution and heat function profile in the collector cannot be shown in any experimental works. The effects of the nanoparticle volume fraction on the isotherm distribution, heat lines, mean Nusselt number, rate of entropy generation, collector efficiency and Bejan number are shown graphically in the present study.

2. MATHEMATICAL FORMULATION

As shown in Figure 1, a two-dimensional heat transfer analysis is developed in which direct sunlight is incident on a thin flowing film of Cu-water nanofluid into a DASC with surface area, length and height of *A*, *L* and *H* respectively. The fluid enters with temperature T_i from left inlet and exits from right port. The bottom wall is considered to be adiabatic. This top surface is assumed to be exposed to the ambient atmosphere and thus loses heat by convection. The thermo-physical properties of the nanoparticle are taken from Ogut (2009) and given in Table 1.

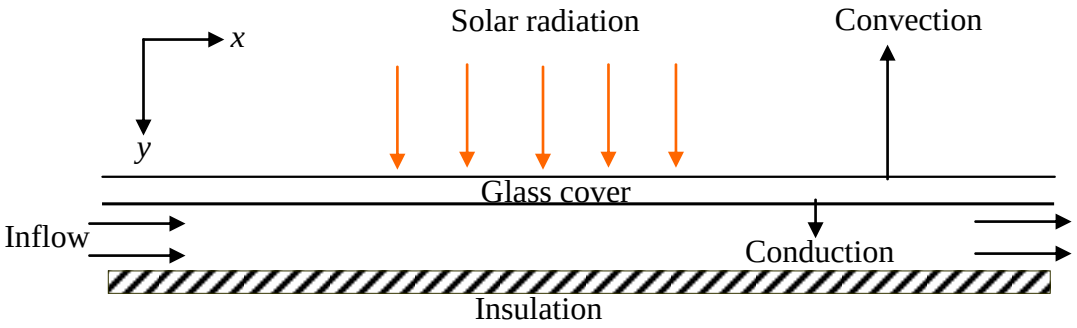

Figure 1. Schematic diagram of the DASC

Table 1. Thermo physical properties of fluid and nanoparticles

PhysicalProperties	Fluid phase(Water)	Cu
C_p(J/kgK)	4179	385
ρ (kg/m^3)	997.1	8933
k (W/mK)	0.613	400
$\alpha\times10^7$ (m^2/s)	1.47	1163.1

The governing equations are

$$\frac{\partial u}{\partial x}+\frac{\partial v}{\partial y}=0, \tag{1}$$

$$\rho_{nf}\left(u\frac{\partial u}{\partial x}+v\frac{\partial u}{\partial y}\right)=-\frac{\partial p}{\partial x}+\mu_{nf}\left(\frac{\partial^2 u}{\partial x^2}+\frac{\partial^2 u}{\partial y^2}\right), \tag{2}$$

$$\rho_{nf}\left(u\frac{\partial v}{\partial x}+v\frac{\partial v}{\partial y}\right)=-\frac{\partial p}{\partial y}+\mu_{nf}\left(\frac{\partial^2 v}{\partial x^2}+\frac{\partial^2 v}{\partial y^2}\right), \tag{3}$$

$$u\frac{\partial T}{\partial x}+v\frac{\partial T}{\partial y}=\alpha_{nf}\left(\frac{\partial^2 T}{\partial x^2}+\frac{\partial^2 T}{\partial y^2}\right)-\left(\frac{1}{\rho C_p}\right)_{nf}\frac{\partial q_r}{\partial y}. \tag{4}$$

The energy equation is coupled to the Radiative Transport Equation (RTE) through the divergence of the radiative flux

$$\frac{\partial q_r}{\partial y} = \int_{\lambda} K_{e\lambda} \tau I_{\lambda} d\lambda \,,$$

where $K_{e\lambda}$ is the extinction coefficient, τ is the transmission coefficient and I_{λ} is the intensity of the solar radiation. Also,

$$\rho_{nf} = (1-\phi)\rho_f + \phi \rho_s$$

is the density,

$$\left(\rho C_p\right)_{nf} = (1-\phi)\left(\rho C_p\right)_f + \phi\left(\rho C_p\right)_s$$

is the heat capacitance and

$$\alpha_{nf} = k_{nf} \Big/ \left(\rho C_p\right)_{nf}$$

is the thermal diffusivity.

In the current study, the viscosity of the nanofluid is considered by the Pak and Cho (1998) correlation. This correlation is given as

$$\mu_{nf} = \mu_f \left(1 + 39.11\phi + 533.9\phi^2\right), \tag{5}$$

and the thermal conductivity of Maxwell Garnett (1904) model is

$$k_{nf} = k_f \frac{k_s + 2k_f - 2\phi\left(k_f - k_s\right)}{k_s + 2k_f + \phi\left(k_f - k_s\right)}. \tag{6}$$

The boundary conditions are:

at all solid boundaries: $u = v = 0$,
at the top surface: inward heat flux per unit area

$$k_{nf} \frac{\partial T}{\partial Y} = q,$$

at the inlet boundary:

$$T = T_{in}\,,\; u = U_{in},$$

at the outlet boundary: convective boundary condition $p = 0$, and
at the bottom surface:

$$\frac{\partial T}{\partial y} = 0.$$

Equations (1) - (4) are non-dimensionalized by using the following dimensionless dependent and independent variables:

$$X = \frac{x}{L}, Y = \frac{y}{L}, U = \frac{u}{U_{in}}, V = \frac{v}{U_{in}}, P = \frac{p}{\rho_f U_{in}^{\ 2}}, \theta = \frac{(T - T_{in})k_f}{qL} \quad (7)$$

.

Then the non-dimensional governing equations are

$$\frac{\partial U}{\partial X} + \frac{\partial V}{\partial Y} = 0, \quad (8)$$

$$U\frac{\partial U}{\partial X} + V\frac{\partial U}{\partial Y} = -\frac{\rho_f}{\rho_{nf}}\frac{\partial P}{\partial X} + \frac{\nu_{nf}}{\nu_f}\frac{1}{Re}\left(\frac{\partial^2 U}{\partial X^2} + \frac{\partial^2 U}{\partial Y^2}\right), \quad (9)$$

$$U\frac{\partial V}{\partial X} + V\frac{\partial V}{\partial Y} = -\frac{\rho_f}{\rho_{nf}}\frac{\partial P}{\partial Y} + \frac{\nu_{nf}}{\nu_f}\frac{1}{Re}\left(\frac{\partial^2 V}{\partial X^2} + \frac{\partial^2 V}{\partial Y^2}\right), \quad (10)$$

$$U\frac{\partial \theta}{\partial X} + V\frac{\partial \theta}{\partial Y} = \frac{1}{RePr}\frac{\alpha_{nf}}{\alpha_f}\left(\frac{\partial^2 \theta}{\partial X^2} + \frac{\partial^2 \theta}{\partial Y^2}\right) - Q, \quad (11)$$

where, $Pr = \frac{\nu_f}{\alpha_f}$ is the Prandtl number, $Re = \frac{U_{in} L}{\nu_f}$ is the Reynolds number and

$$Q = \frac{k_f}{U_i qL\left(\rho C_p\right)_{nf}}\frac{\partial q_r}{\partial Y}$$

is the dimensionless radiative heat flux parameter. The boundary conditions are:

at all solid boundaries:

$$U = V = 0,$$

at the upper wall:

$$\frac{\partial \theta}{\partial Y} = -\frac{k_f}{k_{nf}},$$

at the inlet boundary:

$$\theta = 0, U = 1,$$

at the outlet boundary: convective boundary condition $P = 0$, and
at the bottom wall:

$$\frac{\partial \theta}{\partial Y} = 0.$$

The local and average Nusselt number (Nu) at the top surface can be written as

$$\overline{Nu} = -\frac{k_{nf}}{k_f}\frac{\partial \theta}{\partial Y} \text{ and } Nu = \int_0^1 \overline{Nu}\, dX \text{ , respectively.}$$

Heat function ξ is obtained from conductive heat fluxes $\left(-\frac{\partial \theta}{\partial X}, -\frac{\partial \theta}{\partial Y}\right)$ as well as convective heat fluxes (Uθ, Vθ). It satisfies the steady energy balance equation such that

$$U\theta - \frac{\partial \theta}{\partial X} = \frac{\partial \xi}{\partial Y},\ V\theta - \frac{\partial \theta}{\partial Y} = -\frac{\partial \xi}{\partial X}\ .$$

The non-dimensional entropy generation, S_{gen} can be written by:

$$\begin{aligned} S_{gen} &= s_{gen}\frac{T_0 L^2}{k_f\left(T_{col}-T_{in}\right)^2} \\ &= \frac{k_{nf}}{k_f}\left[\left(\frac{\partial \theta}{\partial X}\right)^2 + \left(\frac{\partial \theta}{\partial Y}\right)^2\right] + \chi\frac{\mu_{nf}}{\mu_f}\left[2\left(\frac{\partial U}{\partial X}\right)^2 + 2\left(\frac{\partial V}{\partial Y}\right)^2 + \left(\frac{\partial U}{\partial X}+\frac{\partial V}{\partial Y}\right)^2\right], \\ &= S_{gen,h} + S_{gen,v}, \end{aligned} \tag{12}$$

where, $S_{gen,\,h}$ and $S_{gen,\,v}$ are the dimensionless entropy generation for heat transfer and viscous effect, respectively. χ is the irreversibility factor.

The dimensionless average entropy generation, S for the entire computational domain is

$$S = \frac{1}{\overline{V}}\int S_{gen}\, d\overline{V} = S_{gen,h,m} + S_{gen,v,m}, \tag{13}$$

where $\overline{V}$ is the volume occupied by the nanofluid.

The Bejan number, *Be* and the collector efficiency (η) are defined as

$$Be = \frac{S_{gen,h,m}}{S} \text{ and } \eta = \frac{\text{useful gain}}{\text{available energy}} = \frac{mC_p\left(T_{out}-T_{in}\right)}{AI},$$

respectively, where, m is the mass flow rate of the fluid flowing through the collector; C_p is the specific heat at constant pressure and T_{in} and T_{out} are the inlet and outlet fluid temperatures, respectively.

3. NUMERICAL IMPLEMENTATION

The Galerkin finite element method is used to solve the non-dimensional governing equations along with boundary conditions for the considered problem. The equation of continuity has

been used as a constraint due to mass conservation and this restriction may be used to find the pressure distribution. The finite element method of Reddy (1994) is used to solve the Equations (8) - (11), where the pressure P is eliminated by a constraint. The continuity equation is automatically fulfilled for large values of this constraint. Then the velocity components (U, V) and temperature (θ) are expanded using a basis set. The Galerkin finite element technique yields the subsequent nonlinear residual equations. Three points Gaussian quadrature is used to evaluate the integrals in these equations. The non-linear residual equations are solved using Newton–Raphson method to determine the coefficients of the expansions. The convergence of solutions is assumed when the relative error for each variable between consecutive iterations is recorded below the convergence criterion such that $\left|\psi^{n+1}-\psi^{n}\right| \le 10^{-4}$, where n is the number of iteration and Ψ is a function of U, V and θ.

4. GRID INDEPENDENT TEST

An extensive mesh testing procedure is conducted to guarantee a grid-independent solution for Re = 600 and Pr = 6.6 in a solar collector. In the present work, we examine five different non-uniform grid systems with the following number of elements within the resolution field: 48, 192, 768, 1616 and 3072. The numerical scheme is carried out for highly precise key in the average Nusselt number for water-Cu nanofluid (ϕ = 3%) as well as base fluid (ϕ = 0%) for the aforesaid elements to develop an understanding of the grid fineness as shown in Table 2. The scale of the average Nusselt numbers for nanofluid and clear water for 1616 elements shows a little difference with the results obtained for the other elements. Hence, considering the non-uniform grid system of 1616 elements is preferred for the computation.

Table 2. Grid Sensitivity Check at Pr = 6.6, ϕ = (3% and 0%) and Re = 600

Nodes (elements)	407 (48)	1434 (192)	5360 (768)	9484 (1616)	20700 (3072)
Nu (nanofluid)	6.10051	7.79143	9.30279	9.992503	10.09242
Nu (basefluid)	5.09253	6.57958	8.19253	8.99084	9.08753
Time (s)	126.265	312.594	398.157	481.328	929.377

5. Results and Discussion

In this section, numerical results of isotherms and heat function for various values of solid volume fraction (ϕ) with Cu/water nanofluid in a direct absorption solar collector are displayed. The considered values of ϕ are ϕ (= 0%, 1%, 3%, 5% and 7%) while the Reynolds number Re = 600, Prandtl number Pr = 6.6, the mass flow rate m = 0.015 (kg/s), solar irradiance I = 1000 W/m^2. In addition, the values of the average Nusselt number, Bejan number, mean entropy generation and percentage of collector efficiency of the DASC are shown graphically.

Figures 2 (a) - (b) represent the effect of ϕ on the thermal and heat flux fields while Re = 600. Isotherms are almost similar to the active parts for water-copper nanofluid. Due to rising values of ϕ, the temperature distributions become distorted resulting in an increase in the

overall heat transfer. This result can be attributed to the dominance of the thermal conductivity property. It is worth noting that as the values of ϕ increase, the thickness of the thermal boundary layer near the top surface rises which indicates a steep temperature gradients and hence, an increase in the overall heat transfer from the hot wall to the nanofluid through the DASC.

The pattern of heat lines is markedly different for various volume fractions. This drastic change in the heat lines pattern should be expected. They are nearly horizontal at the lower portion of the DASC, indicating that convection is not a strong effect so close to the wall. The strong convective-radiative heat transport is seen near the upper and exit boundaries occur for heat lines. Therefore, enhanced thermal mixing occurs at those locations. In contrast, the stratification of heat lines is observed in the domain. The higher density of heat lines near the exit port at ϕ = 3% indicates higher heat fluxes. This remains unchanged with increasing ϕ from 3% to 5%. If we compare them with the water (ϕ = 0%) patterns of Figure 2, we see very clearly that the region occupied by the heat lines becomes thicker as the solid volume fraction increases from 0% to 3%. This agrees very well with the properties of nanofluid. However, the intensity of the radiation is found to be greater in the upper surface.

Figures 3(a)-(b) show average Nusselt number Nu and collector efficiency for the effect of ϕ. Figures 3 (a) displays that *Nu* enhances with growing ϕ up to 3%. Then it remains static for further rising ϕ. The rate of heat transfer for water-copper nanofluid is found to be more effective than the clear water due to higher thermal conductivity of solid nanoparticles. Heat transfer rate rises by 11% for increasing volume fraction from 0% to 3%. Rising solid volume fraction (up to 3%) enhances the collector efficiency. Greater ϕ represents higher thermal conductivity simultaneously higher density properties of the nanofluid. Thus motion of the nanofluid diminishes with enhancing ϕ. So heat transfer phenomena does not improved for further mixing nanoparticles with clear water. About 2 times enhancement of collector efficiency is found in this case.

The variations of average entropy generation and Began number against the solid volume fraction of nanoparticle are displayed in Figures 4 (a)-(b). It is seen that for a fixed value of *Re* = 600, the *S* enhances slightly as the volume fraction of nanoparticles increases up to 3%. This result is to be expected since the addition of a greater number of nanoparticles increases the thermal conductivity and viscosity of the working fluid. The higher thermal conductivity results in a greater temperature gradient within the DASC, and thus the local entropy generation caused by heat transfer irreversibility increases. The greater viscosity of the working fluid increases the local entropy generation due to fluid friction irreversibility. After the level of ϕ = 3%, there is no change in mean entropy generation. It is found from Figure 4 (b)that the heat transfer irreversibility is dominant since *Be* approaches to 1. Increasing *Be* is observed for increasing solid volume fraction of copper nanoparticles within the level 0% to 3%. For further increment of ϕ no variation is found in the Bejan number.

For better understanding the heat transfer and entropy generation the variation of normalized Nusselt number *Nu** and normalized entropy generation *S** against solid volume fraction ϕ are displayed in Figures 5 (a) - (b). *Nu** is the ratio of mean Nusselt number for nanofluid and base fluid where *S** is the ratio of mean entropy generation for nanofluid and base fluid. As in Figure 3 (a), *Nu**-ϕ profile also grows up with the variation of ϕ from 0% to 3%. *S** is also high for higher solid volume fraction up to 3% which is similar to the Figure 4 (a).

5. Conclusions

The influences of solid volume fraction of nanoparticle on forced convection boundary layer flow inside the DASC with water-Cu nanofluid are accounted. The structure of isotherms and heat lines through the solar collector is found to significantly depend upon ϕ. The Cu nanoparticles with ϕ = 3% are established to be most effective in enhancing performance of heat transfer rate. The rate of heat transfer enhances 11% with the variation of ϕ when the collector efficiency enhances almost double for increasing solid volume fraction.

Acknowledgement

The present work is financially supported by the University Grants Commission Bangladesh and is done in the department of mathematics, Bangladesh University of Engineering and Technology.

Nomenclature

A	Surface area of the collector (m^2)
Be	Bejan number
C_p	Specific heat at constant pressure (J kg^{-1} K^{-1})
h	Local heat transfer coefficient (W m^{-2} K^{-1})
I	Intensity of solar radiation(Wm^{-2})
k	Thermal conductivity(W m^{-1} K^{-1})
L	Length of the collector (m)
m	mass flow rate (Kgs^{-1})
Nu	Nusselt number
Pr	Prandtl number
Re	Reynolds number
T	Dimensional temperature (K)
T_{in}	Inputtemperature of fluid (K)
T_{out}	Output temperature of fluid (K)
u, *v*	Dimensional *x*and *y* components of velocity (m s^{-1})
U, *V*	Dimensionless velocities
U_i	Input velocity of fluid (ms^{-1})
X, *Y*	Dimensionless coordinates
x, *y*	Dimensional coordinates (m)
q	Heat flux (Wm^{-2})
V	Dimensionless velocity field

Greek Symbols

α Fluid thermal diffusivity ($m^2\ s^{-1}$)
β Thermal expansion coefficient (K^{-1})
ϕ Nanoparticles volume fraction
ν Kinematic viscosity ($m^2\ s^{-1}$)
η collector efficiency
θ Dimensionless temperature
ρ Density ($kg\ m^{-3}$)
μ Dynamic viscosity ($N\ s\ m^{-2}$)
τ Transmission coefficient

Subscripts

f fluid
nf nanofluid
s solid particle

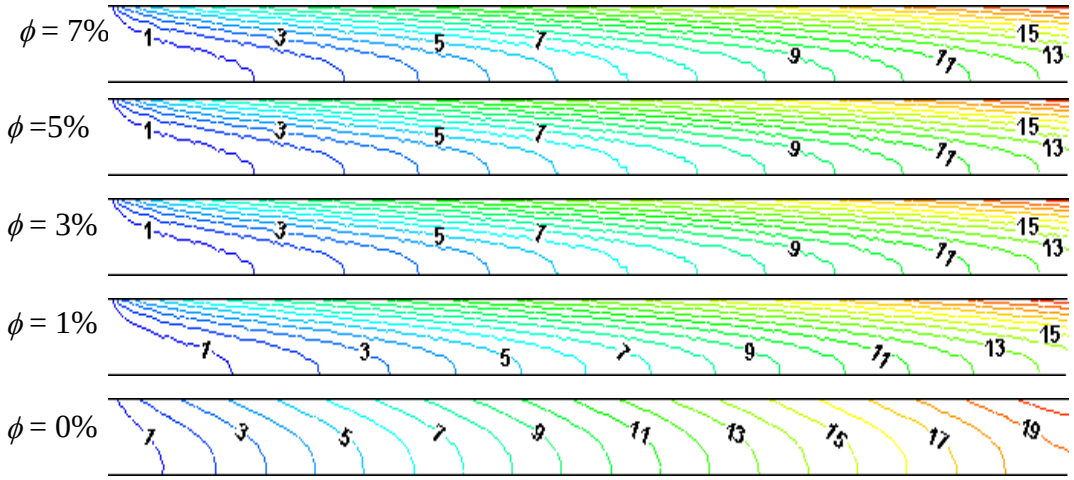

(a) Isotherms

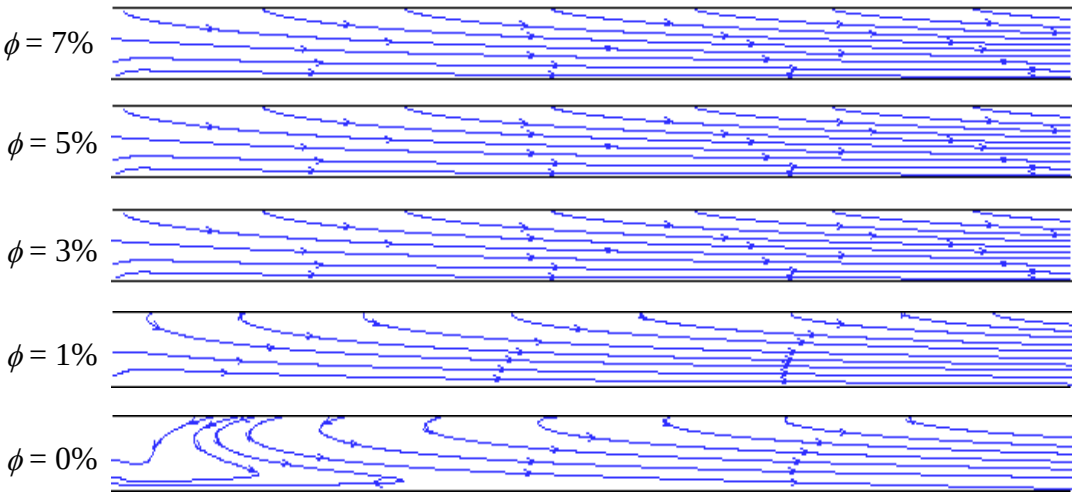

(b) Heat lines

Figure 2. Effect of ϕ on (a) temperature and (b) heat function at *Re* = 600

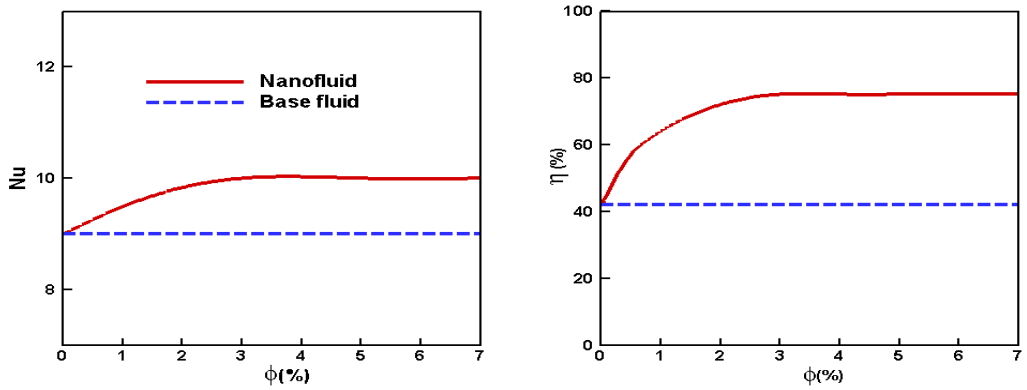

(a) (b)

Figure 3. (a) Average Nusselt number and (b) collector efficiency for the effect of ϕ

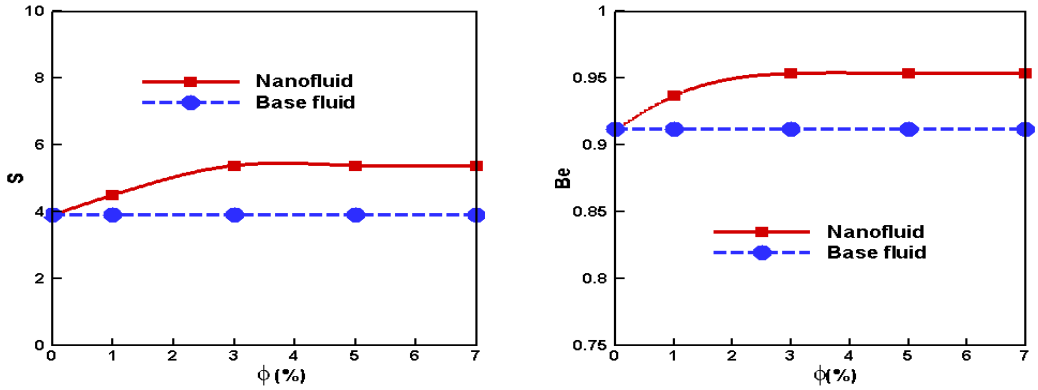

(a) (b)

Figure 4. (a) average entropy generation and (b) Bejan number for the effect of ϕ

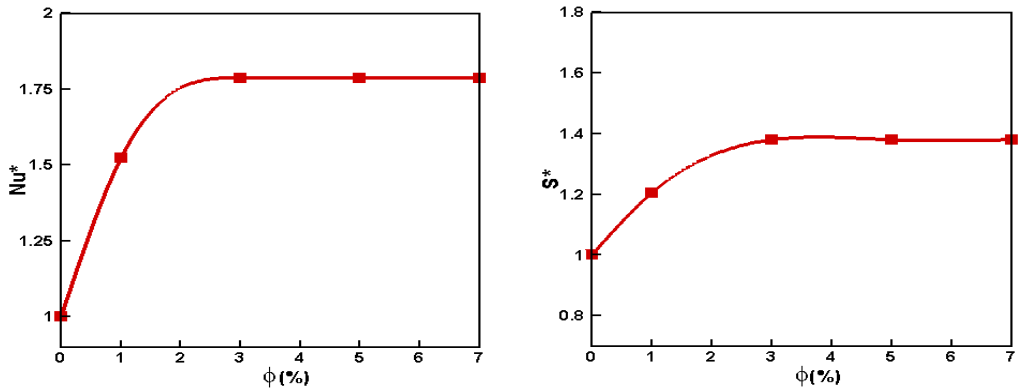

(a) (b)

Figure 5. Normalized (a) Nusselt number and (b) entropy generation for the effect of ϕ

REFERENCES

Álvarez, A., Muñiz, M.C., Varela, L.M., Cabeza, O. (2010). Finite element modelling of a solar collector, Int. Conf. on Renew. Energies and Power Quality, Granada, (Spain).

Basak, T., Aravind, G., Roy, S., Balakrishnan, A.R. (2010). Heat line analysis of heat recovery and thermal transport in materials confined within triangular cavities, Int. J. of Heat and Mass Trans. Vol. 53, pp. 3615–3628.

Bejan A. (1982). Entropy generation through heat and fluid flow. New York: Wiley.

Bejan A. (1996). Entropy generation minimization: the method of thermodynamic optimization of finite-size systems and finite-time processes. Boca Raton: CRC Press.

Delavar, M.A., Hedayatpour, M. (2012). Forced convection and entropy generation inside a channel with a heat-generating porous block, Heat Transfer-Asian Research, Vol. 41, No. 7, pp. 580–600.

Khorasanizadeh, H, Nikfar, M. (2013). Amani J. Entropy generation of Cu–water nanofluid mixed convection in a cavity. Eur J Mech B-Fluid, Vol. 37, pp. 143–152.

Mahian, O., Kianifar, A., Kalogirou, S.A., Pop, I, Wongwises, S. (2013). A review of the applications of nanofluids in solar energy, Int. J. of Heat and Mass Trans. Vol. 57, pp. 582–594.

Maxwell-Garnett, J.C. (1904). Colours in metal glasses and in metallic films. Philos. Trans. Roy. Soc.A,Vol. 203, pp. 385-420.

Morega, AL.M. and Bejan, A. (1993). Heat line visualization of forced convection laminar boundary layers, Int. J. of Heat and Mass Trans. Vol. 36, No. 16, pp. 3957-3966.

Nasrin, R., Parvin, S., Alim, M.A. (2014), Heat Transfer by Nanofluids Through a Flat Plate Solar Collector, Procedia Engineering, 90, pp. 364–370.

Nasrin, R., Parvin, S., Alim, M.A. (2015), Heat transfer and collector efficiency through direct absorption solar collector with radiative heat flux effect, Numerical Heat Transfer, Part A: Application, Vol. 68 No.4, pp. 887-907.

Natarajan, E. & Sathish, R. (2009). Role of nanofluids in solar water heater, Int. J. Adv. Manuf. Techn., Vol. 45, No. 5, pp. DOI 10.1007/s00170-008-1876-8.

Ogut, E.B. (2009). Natural convection of water-based nanofluids in an inclined enclosure with a heat source, Int. J. of Thermal Sci., Vol. 48, No. 11, pp. 2063-2073.

Otanicar, T.P., Phelan, P.E., Prasher, R.S., Rosengarten, G. and Taylor, R.A. (2010). Nanofluid-based direct absorption solar collector, J. of Renew. and Sustain. Energy, Vol.2, pp. 033102.

Pak, B.C., Cho, Y. (1998). Hydrodynamic and heat transfer study of dispersed fluids with submicron metallic oxide particle, Experim. Heat Trans. Vol. 11, pp. 151-170.

Parvin, S., Chamkha, A.J. (2014). An analysis on free convection flow, heat transfer and entropy generation in an odd-shaped cavity filled with nanofluid, Int. Commun. in Heat and Mass Transfer, Vol. 54, pp. 8-17.

Parvin, S., Nasrin, R., Alim, M.A. (2014). Heat transfer and entropy generation through nanofluid filled direct absorption solar collector, International Journal of Heat and Mass Transfer Vol. 71 pp. 386–395.

Reddy, J.N. and Gartling, D.K. (1994).The Finite Element Method in Heat Transfer and Fluid Dynamics, CRC Press, Inc., Boca Raton, Florida.

Taylor A.R, Phelan E.P, Otanicar P.T, Walker A.C, Nguyen M., Trimble S, Ravi P, (2011).Applicability of nanofluids in high flux solar collectors, Int. J. of Renew. and Sust. Energy, Vol. 3, pp. 023104.

Taylor, A.R., Phelan, E.P., Otanicar, P.T, Adrian, R., Prasher, R. (2011). Nanofluid optical property characterization: towards efficient direct absorption solar collectors, Nanoscale Research Letters, Vol. 6, pp. 225.

Tyagi, H., Phelan, P., Prasher, R. (2009). Predicted efficiency of a low-temperature nanofluid-based direct absorption solar collector, J. of Solar Energy Engg., Vol. 131, No. 4, pp. 041004.

Verma, V., Kundan, L. (2013). Thermal performance evaluation of a Direct Absorption Flat Plate Solar Collector (DASC) using Al_2O_3-H_2O based nanofluids, IOSR J. of Mech. and Civil Engg. Vol. 6, No. 2, pp. 29-35.

Zambolin, E. (2011). Theoretical and experimental study of solar thermal collector systems and components, Scuola di Dottorato di Ricerca in Ingegneria Industriale, Indirizzo Fisica Tecnica.